Entanglement evolution and quantum phase transition of biased $s = 1/2$ spin-boson model

Chunjian Zhao, Zhiguo Lü, and Hang Zheng

Key Laboratory of Artificial Structures and Quantum Control (Ministry of Education), Department of Physics, Shanghai Jiao Tong University, Shanghai 200240, China

(Received 28 February 2011; revised manuscript received 25 May 2011; published 11 July 2011)

The ground state and the spectral structure of lower-lying excited states of a dissipative two-level system coupled to a sub-Ohmic bath ($s = 1/2$) with nonzero bias have been studied using the unitary transformation method. By calculating the ground-state entanglement entropy, the ground-state average of $\langle\sigma_z\rangle_G$, and the static susceptibility of the two-level system, we explore the nature of the transition (crossover) between the delocalized and localized state of the two-level system. Furthermore, we calculate the time-dependent expectation $\langle\sigma_z(t)\rangle$ and the time evolution of the entanglement entropy to show that, when the system undergoes a transition (crossover) from the delocalized to the localized state, the time evolution of the two-level system changes from coherent to decoherent dynamics.

DOI: 10.1103/PhysRevE.84.011114 PACS number(s): 05.30.−d, 05.40.−a

I. INTRODUCTION

The physics of a quantum two-level system coupled to a dissipative bosonic environment [spin-boson model (SBM)] has attracted considerable attention in recent years because it provides a universal model for numerous physical and chemical processes [1,2]. The Hamiltonian of the SBM reads (throughout this paper, we set $\hbar = 1$)

$$H = -\frac{1}{2}\Delta\sigma_x + \frac{1}{2}\epsilon\sigma_z + \sum_k \omega_k b_k^\dagger b_k + \frac{1}{2}\sum_k g_k(b_k^\dagger + b_k)\sigma_z, \tag{1}$$

where $b_k^\dagger$ (b_k) is the creation (annihilation) operator of the boson mode with frequency ω_k, σ_x and σ_z are Pauli matrices to describe the two-level system, ϵ is the bias, Δ is the bare tunneling, and g_k is the coupling between spin and environment.

The main theoretical interest in the SBM is to understand how the environment influences the ground state and dynamics of the two-level system and, in particular, how the dissipation effect of the environment destroys quantum coherence. The dynamic properties of the SBM, usually described by the time-dependent expectation $\langle\sigma_z(t)\rangle = \mathrm{Tr}_S\{\mathrm{Tr}_B[\rho_{SB}(t)\sigma_z]\}$ [$\rho_{SB}(t)$ is the density operator for Hamiltonian H and the subscript "SB" indicates that it is for the coupled two-level system and bath], have been studied extensively [1–4]. In this paper, instead of $\langle\sigma_z(t)\rangle$, we consider a quantitative description of the entanglement of the two-level system with the environment and its dynamic evolution, which may be measured by the von Neumann entropy or the entanglement entropy [5–8],

$$E(t) = -\mathrm{Tr}_S[\rho_S(t)\log_2\rho_S(t)] = -p_+(t)\log_2 p_+(t) - p_-(t)\log_2 p_-(t), \tag{2}$$

$$p_\pm(t) = \tfrac{1}{2}\left[1 \pm \sqrt{\langle\sigma_x(t)\rangle^2 + \langle\sigma_y(t)\rangle^2 + \langle\sigma_z(t)\rangle^2}\right], \tag{3}$$

where the subscript "S" of $\rho_S(t)$ means it is the reduced density operator for the two-level system. The dynamic evolution of $E(t)$ is from the initial value $E(0) = 0$ (no entanglement between system and environment because of the initial preparation [4]) at $t = 0$ to the $t \to \infty$ limit $E(\infty) = E(G)$, where the coupled system and environment are in the ground state (G) of H.

The effect of the bosonic environment is characterized by a spectral density $J(\omega) = \sum_k g_k^2\delta(\omega - \omega_k) = 2\alpha\omega^s\omega_c^{1-s}\theta(\omega_c - \omega)$ with the dimensionless coupling strength α and the hard upper cutoff ω_c [$\theta(\omega_c - \omega)$ is the usual step function]. The index s accounts for various physical situations: $s = 1$ is the Ohmic bath [1–4,7] but $s < 1$ stands for the sub-Ohmic bath [1,2,8–11]. As was pointed out by Ref. [8], the case $s = 1/2$ is of particular interest because it may be realized by a charge qubit subject to the electromagnetic noise of an *RLC* transmission line. Another motivation is that, recently, conflicting results have been reported about the critical behavior of the SBM with a sub-Ohmic bath [12].

In the past few years, the numerical renormalization group (NRG) method [8,13–16] and the quantum Monte Carlo method [12] have been used for the sub-Ohmic SBM, and their main focus is to study the properties of the delocalized-localized quantum phase transition. Moreover, based on the noninteracting blip approximation [1], there are claims that the two-level system might be always localized in the sub-Ohmic case for zero temperature, thus there should be no coherent dynamics for the sub-Ohmic bath. Kehrein and Mielke [9] studied the unbiased ($\epsilon = 0$) sub-Ohmic SBM to show that a finite delocalized-localized transition point exists for all $0 < s \leqslant 1$. In our previous work [17], we studied the biased ($\epsilon \neq 0$) sub-Ohmic SBM and focused on how the sub-Ohmic bath influences the dynamics of the two-level system and destroys the quantum coherence. But the renormalization effect of the dissipative interaction (the coupling α) on the effective bias was not taken into account in [17].

As SBM is a quantum many-body system. To study its physical properties, one must first find its correct ground state, which should be an entangled many-body state. Then, the spectral structure of the lower-lying excited states over the ground state may be obtained and it determines the static and dynamic properties of the coupled system and environment. In this work, the analytic approach of Refs. [17–19] is extended to calculate the static and dynamic properties of the SBM with sub-Ohmic bath $s = 1/2$ and finite bias $\epsilon \neq 0$ since this case may be realized in experiment [8]. A new ground state of the SBM, which is different from that of Ref. [17], is derived and the ground-state energy and entanglement entropy are calculated. By comparison with the results of previous papers, we will show that this ground state is quite close to the real ground state. Because both the ground state and the spectral structure of the lower-lying excited states are obtained through our analytic approach, we can calculate the static susceptibility and the time evolution of entanglement. Our results will show that for the $s = 1/2$ sub-Ohmic bath, a nonzero bias plays an important role in determining the static properties and quantum dynamics of the SBM.

II. ENTANGLEMENT IN THE GROUND STATE

To find the ground state of the correlated system of spin and bosons, we present a treatment based on the unitary transformation approach [17,19,20]: $H' = \exp(S)H\exp(-S)$, with the generator

$$S = \sum_k \frac{g_k}{2\omega_k}(b_k^\dagger - b_k)[\xi_k\sigma_z + (1-\xi_k)\sigma_0]. \tag{4}$$

Here we introduce in S a constant σ_0 and a k-dependent function ξ_k; their form will be determined later. The transformation can be done to the end and the result is

$$H' = H_0' + H_1' + H_2', \tag{5}$$

$$\begin{aligned} H_0' = &-\frac{1}{2}\eta\Delta\sigma_x + \frac{1}{2}\left[\epsilon - \sum_k \frac{g_k^2}{\omega_k}\sigma_0(1-\xi_k)^2\right]\sigma_z \\ &+ \sum_k \omega_k b_k^\dagger b_k - \sum_k \frac{g_k^2}{4\omega_k}\xi_k(2-\xi_k) \\ &+ \sum_k \frac{g_k^2}{4\omega_k}\sigma_0^2(1-\xi_k)^2, \end{aligned} \tag{6}$$

$$\begin{aligned} H_1' = &\frac{1}{2}\sum_k g_k(1-\xi_k)(b_k^\dagger + b_k)(\sigma_z - \sigma_0) \\ &-\frac{1}{2}\eta\Delta i\sigma_y \sum_k \frac{g_k}{\omega_k}\xi_k(b_k^\dagger - b_k), \end{aligned} \tag{7}$$

$$\begin{aligned} H_2' = &-\frac{1}{2}\Delta\sigma_x\left(\cosh\left\{\sum_k \frac{g_k}{\omega_k}\xi_k(b_k^\dagger - b_k)\right\} - \eta\right) \\ &-\frac{1}{2}\Delta i\sigma_y\left(\sinh\left\{\sum_k \frac{g_k}{\omega_k}\xi_k(b_k^\dagger - b_k)\right\}\right. \\ &\left.-\eta\sum_k \frac{g_k}{\omega_k}\xi_k(b_k^\dagger - b_k)\right), \end{aligned} \tag{8}$$

where

$$\begin{aligned} \eta &= \langle\{0_k\}|\cosh\left\{\sum_k \frac{g_k}{\omega_k}\xi_k(b_k^\dagger - b_k)\right\}|\{0_k\}\rangle \\ &= \exp\left[-\sum_k \frac{g_k^2}{2\omega_k^2}\xi_k^2\right] \end{aligned} \tag{9}$$

is an average over the vacuum state of the bath $|\{0_k\}\rangle$. Note that in Ref. [17], the second term in H_0' is $\frac{1}{2}\epsilon\sigma_z$ and the fifth term is $-\sum_k \frac{g_k^2}{4\omega_k}\sigma_0^2(1-\xi_k)^2$, but there is an extra term in H_2': $-\sum_k \frac{g_k^2}{2\omega_k}\sigma_0(1-\xi_k)^2(\sigma_z - \sigma_0)$. This difference leads to a different ground state and different physical properties from those of Ref. [17]. We show the difference below.

Obviously, in H_0' the spin and bosons are decoupled and its spin part can be diagonalized by a unitary matrix U,

$$U = \begin{pmatrix} u & v \\ v & -u \end{pmatrix}, \tag{10}$$

$$u = \frac{1}{\sqrt{2}}\left(1 - \frac{\epsilon'}{W}\right)^{1/2}, \quad v = \frac{1}{\sqrt{2}}\left(1 + \frac{\epsilon'}{W}\right)^{1/2}, \tag{11}$$

where $W = [\epsilon'^2 + \eta^2\Delta^2]^{1/2}$ and $\epsilon' = \epsilon - \sum_k \frac{g_k^2}{\omega_k}\sigma_0(1-\xi_k)^2$ is the effective bias renormalized by the dissipative interaction α. The diagonalized H_0' is

$$\begin{aligned} \tilde{H}_0 = U^\dagger H_0' U = &-\frac{1}{2}W\sigma_z + \sum_k \omega_k b_k^\dagger b_k \\ &- \sum_k \frac{g_k^2}{4\omega_k}\xi_k(2-\xi_k) + \sum_k \frac{g_k^2}{4\omega_k}\sigma_0^2(1-\xi_k)^2. \end{aligned} \tag{12}$$

The first-order term H_1' is transformed by the unitary matrix as follows:

$$\begin{aligned} \tilde{H}_1 &= U^\dagger H_1' U \\ &= -\frac{1}{2}\sum_k g_k(1-\xi_k)(b_k^\dagger + b_k)\left[\frac{\epsilon'}{W}\sigma_z + \sigma_0\right] \\ &\quad + \frac{\eta\Delta}{2W}\sigma_x \sum_k g_k(1-\xi_k)(b_k^\dagger + b_k) \\ &\quad + \frac{1}{2}\eta\Delta i\sigma_y \sum_k \frac{g_k}{\omega_k}\xi_k(b_k^\dagger - b_k). \end{aligned} \tag{13}$$

H_2' is transformed as $\tilde{H}_2 = U^\dagger H_2' U$ and the total Hamiltonian after transformation is $\tilde{H} = \tilde{H}_0 + \tilde{H}_1 + \tilde{H}_2$. Up to now, the transformation has been done exactly and there is no approximation.

The eigenstate of $\tilde{H}_0$ is a direct product: $|s\rangle|\{n_k\}\rangle$, where $|s\rangle$ is the eigenstate of σ_z: $|s_1\rangle = \binom{1}{0}$ or $|s_2\rangle = \binom{0}{1}$, and $|\{n_k\}\rangle$ is the eigenstate of bosons with n_k phonons for mode k. In particular, $|\{0_k\}\rangle$ is the vacuum state in which $n_k = 0$ for every k. It is easy to check that the ground state of $\tilde{H}_0$ is

$$|\tilde{G}\rangle = |s_1\rangle|\{0_k\}\rangle. \tag{14}$$

To make $|\tilde{G}\rangle$ be the ground state of $\tilde{H}_0 + \tilde{H}_1$, σ_0 and ξ_k should be determined in such a way that

$$\sigma_0 = -\frac{\epsilon'}{W}, \tag{15}$$

$$\xi_k = \frac{\omega_k}{\omega_k + W}, \tag{16}$$

so that

$$\begin{aligned} \tilde{H}_1 = &\frac{1}{2}\sum_k g_k(1-\xi_k)(b_k^\dagger + b_k)\frac{\epsilon'}{W}[1-\sigma_z] \\ &+ \frac{1}{2}\eta\Delta\sum_k \frac{g_k}{\omega_k}\xi_k[b_k^\dagger(\sigma_x + i\sigma_y) + b_k(\sigma_x - i\sigma_y)] \end{aligned}$$

$$= \frac{1}{2}(1-\sigma_z)\sum_k Q_k(b_k^\dagger + b_k) + \frac{1}{2}\sum_k V_k[b_k^\dagger(\sigma_x + i\sigma_y) + b_k(\sigma_x - i\sigma_y)], \quad (17)$$

where $Q_k = \lambda_k\epsilon'$, $V_k = \lambda_k\eta\Delta$, and $\lambda_k = g_k/(\omega_k + W)$. Thus, $\tilde{H}_1|\tilde{G}\rangle = 0$ and $|\tilde{G}\rangle$ is the ground state of $\tilde{H}_0 + \tilde{H}_1$, $(\tilde{H}_0 + \tilde{H}_1)|\tilde{G}\rangle = E_g|\tilde{G}\rangle$, with the ground-state energy

$$E_g = -\frac{1}{2}W - \sum_k \frac{g_k^2}{4\omega_k}\xi_k(2-\xi_k) + \sum_k \frac{g_k^2}{4\omega_k}\sigma_0^2(1-\xi_k)^2. \quad (18)$$

It can be checked that Eqs. (15) and (16) can be derived from the following minimum conditions for E_g:

$$\frac{\partial E_g}{\partial \sigma_0} = 0 \quad \text{and} \quad \frac{\partial E_g}{\partial \xi_k} = 0. \quad (19)$$

Figure 1 shows our calculated E_g as a function of Δ for $s = 1/2$, $\alpha = 0.1$, and $\epsilon/\omega_c = 0.01$. For comparison, we also show the difference between E_g of this work and those of Refs. [17] and [21]: $\delta E_g = E_g^{[17]} - E_g$ and $\delta E_g = E_g^{[21]} - E_g$. Obviously, E_g of this work is lower than previous ones, which is an indication that the ground state of this work is much closer to the real ground state.

In this work, the main approximation is to approximate the transformed Hamiltonian as $\tilde{H} \approx \tilde{H}_0 + \tilde{H}_1$ with the ground state $|\tilde{G}\rangle$ Eq. (14) and its energy E_g Eq. (18). The reason this approximation is justified is that, since $\langle\tilde{G}|\tilde{H}_2|\tilde{G}\rangle = 0$ (because of the definition for η Eq. (9)), the terms in $\tilde{H}_2$ are related to the multiboson nondiagonal transitions (like $b_k b_{k'}$ and $b_k^\dagger b_{k'}^\dagger$). The contributions of these nondiagonal terms to the ground-state energy are $O(g_k^2 g_{k'}^2)$ and higher. For the zero-temperature case, the contribution from these multiboson nondiagonal transition may be dropped safely.

As $|\tilde{G}\rangle$ is the approximate ground state of $\tilde{H}$, the approximate ground state for the original Hamiltonian H is $|G\rangle = e^{-S}U|\tilde{G}\rangle$ with the same ground-state energy E_g. Besides, the ground-state averages $\langle\sigma_x\rangle_G = \langle G|\sigma_x|G\rangle$ and $\langle\sigma_z\rangle_G = \langle G|\sigma_z|G\rangle$ can be calculated by the following differentials of the ground-state energy:

$$\langle\sigma_x\rangle_G = \frac{-2\partial E_g}{\partial\Delta} \quad \text{and} \quad \langle\sigma_z\rangle_G = \frac{2\partial E_g}{\partial\epsilon}. \quad (20)$$

The differentials in (20) can be done easily with the results

$$\langle\sigma_x\rangle_G = \eta^2\Delta/W \quad \text{and} \quad \langle\sigma_z\rangle_G = -\epsilon'/W. \quad (21)$$

According to Eqs. (2) and (3), the ground-state entanglement entropy is

$$E(G) = -p_+(G)\log_2 p_+(G) - p_-(G)\log_2 p_-(G), \quad (22)$$

$$p_\pm(G) = \tfrac{1}{2}[1 \pm \sqrt{\langle\sigma_x\rangle_G^2 + \langle\sigma_z\rangle_G^2}], \quad (23)$$

since $\langle\sigma_y\rangle_G = 0$ as H is invariant under $\sigma_y \to -\sigma_y$. First, we check the entanglement in some limiting cases. When $\alpha = 0$, there is no coupling between the two-level system and environment, and we have $\eta = 1$, $\epsilon' = \epsilon$, $W = \sqrt{\Delta^2 + \epsilon^2}$, and $E(G,\alpha = 0) = 0$. When $\Delta = 0$ but ϵ is finite, there is no quantum tunneling in the original Hamiltonian (1), and we have $\langle\sigma_x\rangle_G = 0$, $\langle\sigma_z\rangle_G = -1$, and $E(G,\Delta = 0) = 0$. When $\Delta = \epsilon = 0$, Eqs. (22) and (23) lead to $E(G) = 1$, which is not correct [this comes from the fact that Hamiltonian (1) is undetermined when $\Delta = \epsilon = 0$]. In the following numerical calculations for entanglement entropy, we will keep a finite value for ϵ, even if it may be very small.

Figure 2 shows our calculated $E(G)$ as a function of Δ for the same case as that of Fig. 1. For comparison, the results of the NRG [8] and of Refs. [17] and [21] are also shown. It is obvious that the curve of this work is quite close to that of the NRG [8], but those of Refs. [17,21] are not. Figure 3 shows our calculated $E(G)$ as functions of Δ for $s = 1/2$, $\alpha = 0.1$, and several values of ϵ. For comparison, the results of the NRG are also shown. The corresponding curves are quantitatively quite close, especially the curves for very small $\epsilon/\omega_c = 10^{-5}$, which are of the same cusp structure at the maximum of entanglement

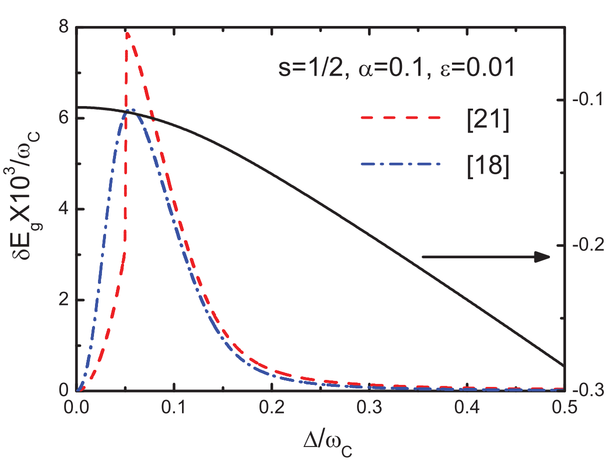

FIG. 1. (Color online) E_g of this work as a function of Δ for $s = 1/2$, $\alpha = 0.1$, and $\epsilon/\omega_c = 0.01$ (solid line, right scale). For comparison, we also show the difference between E_g of this work and those of [17] (dashed-dotted line) and [21] (dashed line): $\delta E_g = E_g^{[17]} - E_g$ and $\delta E_g = E_g^{[21]} - E_g$.

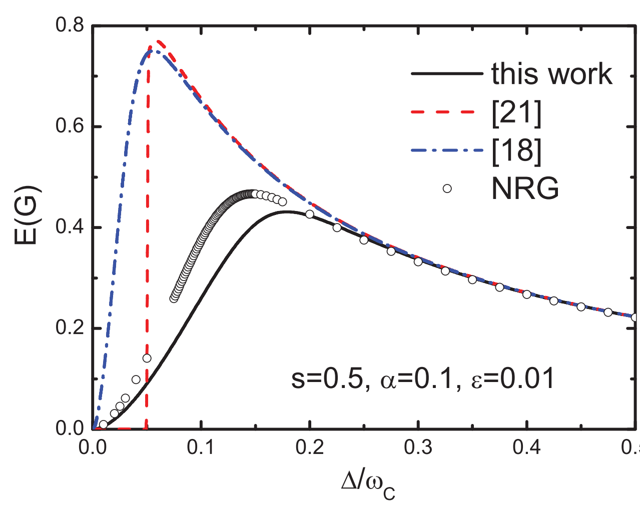

FIG. 2. (Color online) $E(G)$ of this work as a function of Δ for the same case as that of Fig. 1. For comparison, the results of the NRG [8] (circle), of [17] (dashed-dotted line), and of [21] (dashed line) are also shown.

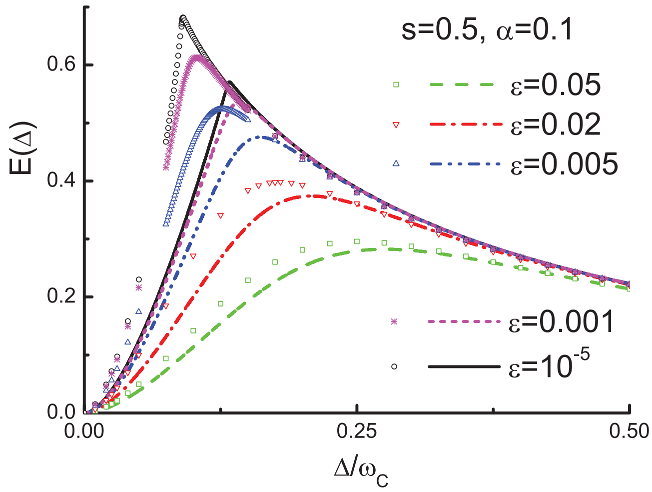

FIG. 3. (Color online) $E(G)$ of this work (lines) as functions of Δ for $s=1/2$, $\alpha=0.1$, and several values of ϵ. For comparison, the results of the NRG (symbols) are also shown.

entropy. These comparisons of our calculated $E(G)$ with the result of the NRG [8] are evidence that our ground state is quite close to the real ground state.

In Fig. 4, we show $E(G)$ as functions of α for $s=1/2$, $\Delta/\omega_c=0.1$, and several values of ϵ. Note that there is also a cusp structure at the maximum of entanglement entropy for very small $\epsilon/\omega_c=10^{-5}$, but for larger ϵ there is a smooth maximum. We note that the cusp on the curve of $\epsilon/\omega_c=10^{-5}$ is at $\alpha=0.0855$.

LeHur *et al.* [8] claimed that the cusp (maximum) in the entanglement entropy versus the Δ (α) relation is an indication of a second-order quantum phase transition separating a delocalized and a localized phase for the spin. The nature of this phase transition may be shown by calculating $\langle\sigma_z\rangle_G$ and $\langle\sigma_x\rangle_G$ separately; see Fig. 5. For very small bias ($\epsilon/\omega_c=10^{-5}$ in Fig. 5), there is a transition at around $\alpha=\alpha_c=0.0855$ (the same place as that of the cusp in Fig. 4): $\langle\sigma_z\rangle_G$ is nearly zero

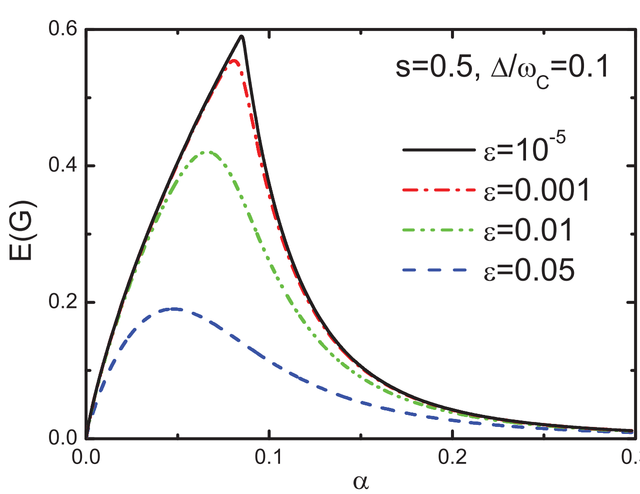

FIG. 4. (Color online) $E(G)$ as functions of α for $s=1/2$, $\Delta/\omega_c=0.1$, and several values of ϵ. The cusp on the curve of $\epsilon/\omega_c=10^{-5}$ is at $\alpha=0.0855$.

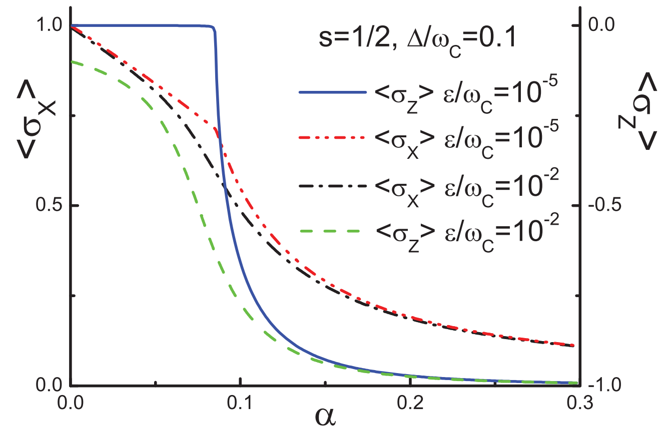

FIG. 5. (Color online) $\langle\sigma_x\rangle_G$ and $\langle\sigma_z\rangle_G$ as functions of α for $\epsilon/\omega_c=10^{-2}$ and 10^{-5}.

for $\alpha<\alpha_c$ and there is a kink at around α_c; for larger $\alpha>\alpha_c$, $\langle\sigma_z\rangle_G$ decreases quickly to $\langle\sigma_z\rangle_G\to-1$ (solid line in Fig. 5). In addition, $\langle\sigma_x\rangle_G$ decreases smoothly (dashed-double-dotted line in Fig. 5) with a small change of its slope at around $\alpha=\alpha_c=0.0855$. For larger bias ($\epsilon/\omega_c=10^{-2}$ in Fig. 5), the transition is smoothed out and there is a crossover of the value of $\langle\sigma_z\rangle_G$ from close to zero to -1 (dashed line in Fig. 5).

The transition at $\alpha\approx\alpha_c$ in Fig. 5 from $\langle\sigma_z\rangle_G\approx 0$ to $\langle\sigma_z\rangle_G\to-1$ comes from the renormalization of the effective bias,

$$\epsilon'=\epsilon\Bigg/\left[1-\sum_k\frac{g_k^2}{\omega_k W}(1-\xi_k)^2\right], \tag{24}$$

where Eq. (15) is used. One can see from this equation that the effective bias $\epsilon'>\epsilon$ for finite coupling α and in our calculations ϵ' is determined self-consistently. The nature of this transition will be discussed further in the next section.

III. SUSCEPTIBILITY AND DELOCALIZED-LOCALIZED TRANSITION

In the preceding section, the ground-state averages of operators were calculated where the first order $\tilde{H}_1$ does nothing because $\tilde{H}_1|\tilde{G}\rangle=0$. In this section, we calculate the time correlation function in the ground state and its Fourier transformation, the susceptibility, where $\tilde{H}_1$ should play important roles. In Ref. [17], we derived the expressions for the time correlation function and the imaginary part of the susceptibility,

$$\begin{aligned}\chi''(\omega)&=\int_{-\infty}^{\infty}dt\,\exp(i\omega t)\\&\quad\times\frac{1}{2}\langle G|[e^{iHt}\sigma_z e^{-iHt}\sigma_z-\sigma_z e^{iHt}\sigma_z e^{-iHt}]|G\rangle\\&=\frac{(\eta\Delta)^2}{W^2}\left\{\frac{\Gamma(\omega)\theta(\omega)}{[\omega-W-\Sigma(\omega)]^2+\Gamma^2(\omega)}\right.\\&\quad\left.-\frac{\Gamma(-\omega)\theta(-\omega)}{[\omega+W+\Sigma(-\omega)]^2+\Gamma^2(-\omega)}\right\},\end{aligned} \tag{25}$$

where

$$\Gamma(\omega) = \gamma(\omega) + \frac{\epsilon^2}{\eta^2\Delta^2}\gamma(\omega - W), \tag{26}$$

$$\Sigma(\omega) = R(\omega) + \frac{\epsilon^2}{\eta^2\Delta^2}R(\omega - W). \tag{27}$$

Here $R(\omega)$ and $\gamma(\omega)$ are contributions from the first order $\tilde{H}_1$, which are real and imaginary parts of $\sum_k V_k^2/(\omega - i0^+ - \omega_k)$ [note that V_k is the coefficient in $\tilde{H}_1$, Eq. (17)],

$$R(\omega) = (\eta\Delta)^2 \sum_{\mathbf{k}} \frac{\lambda_k^2}{(\omega - \omega_{\mathbf{k}})} = (\eta\Delta)^2 \int_0^\infty d\omega' \frac{J(\omega')}{(\omega - \omega')(\omega' + W)^2}, \tag{28}$$

$$\gamma(\omega) = \pi(\eta\Delta)^2 \sum_{\mathbf{k}} \lambda_k^2 \delta(\omega - \omega_{\mathbf{k}}) = \frac{\pi J(\omega)(\eta\Delta)^2}{(\omega + W)^2}. \tag{29}$$

$J(\omega) = 2\alpha\sqrt{\omega\omega_c}\theta(\omega_c - \omega)$ is the spectral density for the $s = 1/2$ bath.

The static susceptibility $\chi'(\omega = 0)$ can be obtained by the following integral:

$$\chi'(\omega = 0) = \frac{2}{\pi}\int_0^\infty \frac{\chi''(\omega)}{\omega} d\omega. \tag{30}$$

Figure 6 shows the static susceptibility $\chi'(0)$ as functions of Δ for $s = 1/2$, $\alpha = 0.1$, and several values of ϵ. One can see that there is a sharp peak of the curve for very small $\epsilon/\omega_c = 10^{-5}$, and the peak position (around $\Delta/\omega_c \approx 0.133$) is at the same place as the cusp maximum of the $E(G)$ versus Δ relation in Fig. 3. Figure 7 shows $\chi'(0)$ as functions of α for $s = 1/2$, $\Delta/\omega_c = 0.1$, and several values of ϵ. A sharp peak of the curve exists for very small $\epsilon/\omega_c = 10^{-5}$, and the peak position (around $\alpha \approx 0.0855$) is at the same place as both the cusp maximum of the $E(G)$ versus α relation in Fig. 4 and the transition point $\alpha_c = 0.0855$ in Fig. 5.

The sharp peak on the curves for $\epsilon/\omega_c = 10^{-5}$ in Figs. 6 and 7 is an indication that there is a transition of the state

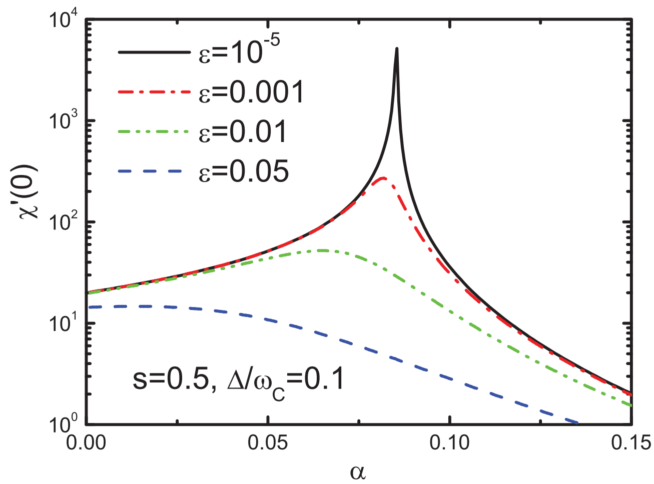

FIG. 7. (Color online) $\chi'(0)$ as functions of α for $s = 1/2$, $\Delta/\omega_c = 0.1$, and several values of ϵ.

of the coupled two-level system and environment at $\Delta/\omega_c \approx 0.133$ when $\alpha = 0.1$ or at $\alpha \approx 0.0855$ when $\Delta/\omega_c = 0.1$. As is shown in Figs. 5 and 7, the transition is very similar to the appearance of the Anderson localized magnetic moment in the famous Anderson model [22] when the Coulomb repulsion on the impurity site is larger than some critical value. The static susceptibility of the Anderson model is divergent at the critical point. Figure 8 is a "phase diagram" of the different regimes in the $s = 1/2$ SBM when the finite bias is very small, $\epsilon/\omega_c = 10^{-5}$. The solid line separates the localized from the delocalized state. A similar "phase diagram" was presented in Ref. [6] by a qualitative discussion.

For larger ϵ, the peaks of susceptibility in Figs. 6 and 7 become smoother and smoother (note the logarithmic scale of the vertical axis), which indicates that for larger ϵ there may not be a sharp transition but rather a crossover between the delocalized and localized state.

In our approach, the main approximation we made is the omission of $\tilde{H}_2$. Hence, the validity of our approach should be

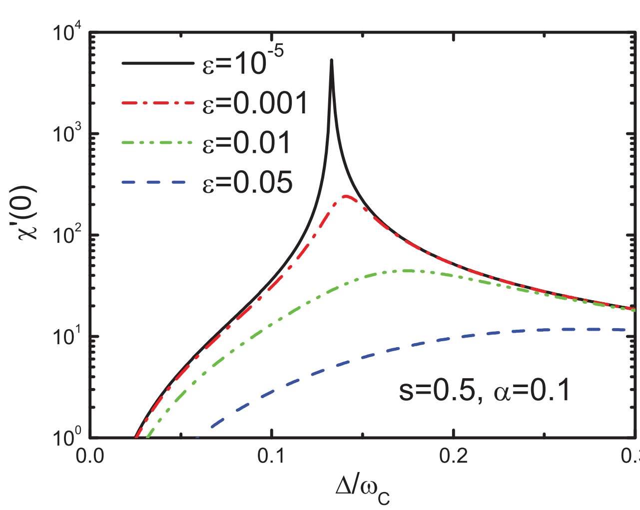

FIG. 6. (Color online) $\chi'(0)$ as functions of Δ for $s = 1/2$, $\alpha = 0.1$, and several values of ϵ.

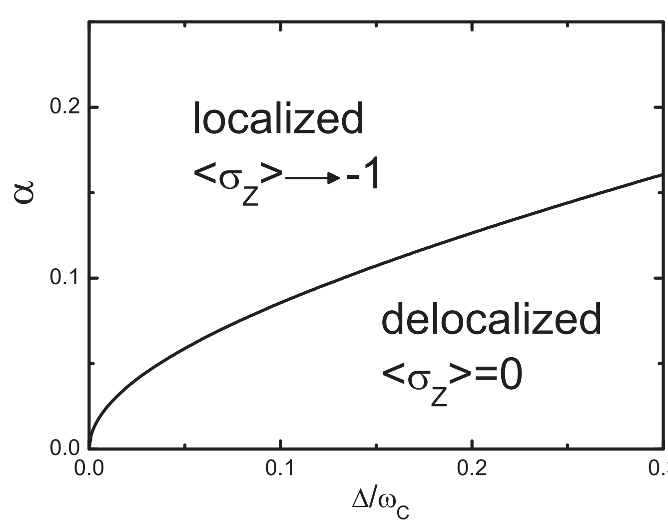

FIG. 8. "Phase diagram" of the different regimes in the $s = 1/2$ SBM when the finite bias is very small, $\epsilon/\omega_c = 10^{-5}$. The solid line separates the delocalized from the localized regime.

checked, and one way to justify our approach is with Shiba's relation [3,23,24],

$$\lim_{\omega\to 0}\frac{\chi''(\omega)}{J(\omega)}=\frac{\pi}{4}[\chi'(\omega=0)]^2, \tag{31}$$

which should be satisfied for the two-level system coupled to a heat bath. We have checked this relation and it is satisfied for all the cases we calculated with error less than 10^{-4} [17,18].

IV. TIME EVOLUTION OF THE ENTANGLEMENT

Time evolution may be the most interesting problem for the quantum two-level system interacting with the dissipative environment and from which one can check whether the quantum dynamics is coherent or decoherent. The time-dependent density operator for the coupled two-level system and bath is $\rho_{SB}(t)$: $\rho_{SB}(t)=e^{-iHT}\rho_{SB}(0)e^{iHt}$, where $\rho_{SB}(0)$ is the initial density operator and the evolution is governed by Hamiltonian H [25]. For the transformed Hamiltonian $\tilde{H}$, the density operator is $\tilde{\rho}_{SB}(t)=U^\dagger e^S\rho_{SB}(t)e^{-S}U$. In Ref. [17], we have derived the master equation for the matrix elements of the density operator,

$$\tilde{\rho}_S(t)=\mathrm{Tr}_B\tilde{\rho}_{SB}(t)=\begin{pmatrix}\tilde{\rho}_{11}(t) & \tilde{\rho}_{12}(t)\\ \tilde{\rho}_{21}(t) & \tilde{\rho}_{22}(t)\end{pmatrix}, \tag{32}$$

$$\frac{d}{dt}\tilde{\rho}_{22}(t)=-\int_0^t dt'\sum_{\mathbf{k}}V_{\mathbf{k}}^2[e^{i(\omega_{\mathbf{k}}-W)(t-t')}+e^{-i(\omega_{\mathbf{k}}-W)(t-t')}]\tilde{\rho}_{22}(t'), \tag{33}$$

$$\frac{d}{dt}\tilde{\rho}_{21}(t)=-iW\tilde{\rho}_{21}(t)-\int_0^t dt'\sum_k\left[Q_k^2e^{-i(\omega_k+W)(t-t')}+V_k^2e^{-i\omega_k(t-t')}\right]\tilde{\rho}_{21}(t'). \tag{34}$$

Another two elements are $\tilde{\rho}_{11}(t)=1-\tilde{\rho}_{22}(t)$ and $\tilde{\rho}_{12}(t)=[\tilde{\rho}_{21}(t)]^\dagger$. The master equation has been solved by the Born approximation and its details are listed in Ref. [17]. Here we show the main results. Equations (33) and (34) have been solved by means of the Laplace transformation, and the solution can be expressed by integration,

$$\tilde{\rho}_{22}(t)=\frac{\tilde{\rho}_{22}(0)}{2\pi}\int_{-\infty}^{\infty}\frac{i\exp(-i\omega t)d\omega}{\omega-[R(W+\omega)-R(W-\omega)]+i[\gamma(W+\omega)+\gamma(W-\omega)]}, \tag{35}$$

$$\tilde{\rho}_{21}(t)=\frac{\tilde{\rho}_{21}(0)}{2\pi}\int_{-\infty}^{\infty}\frac{i\exp(-i\omega t)d\omega}{\omega-W-\Sigma(\omega)+i\Gamma(\omega)}. \tag{36}$$

The expressions for $\Gamma(\omega)$, $\Sigma(\omega)$, $R(\omega)$, and $\gamma(\omega)$ are listed in Eqs. (26)–(29).

$\tilde{\rho}_{21}(0)$ and $\tilde{\rho}_{22}(0)$ in Eqs. (35) and (36) are the initial density operator of the system at $t=0$. First, let us see if the coupled system and environment are initially in the ground state $|G\rangle$. Then $\rho_{SB}(0)=|G\rangle\langle G|=e^{-S}U|\tilde{G}\rangle\langle\tilde{G}|U^\dagger e^S$ and $\tilde{\rho}_{SB}(0)=|\tilde{G}\rangle\langle\tilde{G}|=\left(\begin{smallmatrix}1&0\\0&0\end{smallmatrix}\right)|\{0_k\}\rangle\langle\{0_k\}|$ with $\tilde{\rho}_{21}(0)=0$ and $\tilde{\rho}_{22}(0)=0$. Equations (35) and (36) lead to $\tilde{\rho}_{21}(t)=0$ and $\tilde{\rho}_{22}(t)=0$ for all $t>0$, that is, the system is always in the ground state. This is reasonable since the ground state does not evolve.

Second, if the initial density operator is $\rho_{SB}(0)=e^{-S}\left(\begin{smallmatrix}1&0\\0&0\end{smallmatrix}\right)|\{0_k\}\rangle\langle\{0_k\}|e^S$ and the initial reduced density operator is $\rho_S(0)=\mathrm{Tr}_B\rho_{SB}(0)=\left(\begin{smallmatrix}1&0\\0&0\end{smallmatrix}\right)$, the initial value of the entanglement entropy is $E(0)=0$, which means that by initial preparation [4] we start from the zero entanglement state of the coupled two-level system and environment. For Eqs. (35) and (36), we need the corresponding initial reduced density operator for $\tilde{H}$,

$$\tilde{\rho}_S(0)=\tfrac{1}{2}\begin{pmatrix}1-\epsilon'/W & \eta\Delta/W\\ \eta\Delta/W & 1+\epsilon'/W\end{pmatrix}. \tag{37}$$

To calculate the time-dependent entanglement entropy, according to Eqs. (2) and (3), the following time-dependent expectation values should be calculated: $\langle\sigma_{z(x,y)}(t)\rangle=\mathrm{Tr}_S\{\mathrm{Tr}_B[\rho_{SB}(t)\sigma_{z(x,y)}]\}$. Because of the unitary transforms, the calculation proceeds as follows [17]:

$$\begin{aligned}\langle\sigma_z(t)\rangle&=\mathrm{Tr}_S\{\mathrm{Tr}_B[e^{-S}U\tilde{\rho}_{SB}(t)U^\dagger e^S\sigma_z]\}\\&=\mathrm{Tr}_S\left(\tilde{\rho}_S(t)\left[-\frac{\epsilon'}{W}\sigma_z+\frac{\eta\Delta}{W}\sigma_x\right]\right)\\&=\frac{\epsilon'}{W}[2\tilde{\rho}_{22}(t)-1]+\frac{2\eta\Delta}{W}\mathrm{Re}[\tilde{\rho}_{21}(t)],\end{aligned} \tag{38}$$

$$\begin{aligned}\langle\sigma_x(t)\rangle&=\mathrm{Tr}_S\{\mathrm{Tr}_B[e^{-S}U\tilde{\rho}_{SB}(t)U^\dagger e^S\sigma_x]\}\\&=\mathrm{Tr}_S\left(\tilde{\rho}_S(t)\eta\left[\frac{\epsilon'}{W}\sigma_x+\frac{\eta\Delta}{W}\sigma_z\right]\right)\\&=\frac{2\eta\epsilon'}{W}\mathrm{Re}[\tilde{\rho}_{21}(t)]-\frac{\eta^2\Delta}{W}[2\tilde{\rho}_{22}(t)-1],\end{aligned} \tag{39}$$

$$\begin{aligned}\langle\sigma_y(t)\rangle&=\mathrm{Tr}_S\{\mathrm{Tr}_B[e^{-S}U\tilde{\rho}_{SB}(t)U^\dagger e^S\sigma_y]\}\\&=-\eta\mathrm{Tr}_S[\tilde{\rho}_S(t)\sigma_y]=-2\eta\,\mathrm{Im}[\tilde{\rho}_{21}(t)].\end{aligned} \tag{40}$$

The equations for $\tilde{\rho}_{22}(t)$ and $\tilde{\rho}_{21}(t)$ are (35) and (36) and the results can be obtained by numerical integration with sub-Ohmic spectral density.

Figure 9 shows the time evolution of the usual time-dependent expectation [1,2,17] $P(t)=\langle\sigma_z(t)\rangle$ for $s=1/2$, $\Delta/\omega_c=0.1$, $\epsilon/\omega_c=10^{-5}$, and several values of α. Since $\epsilon/\Delta=10^{-4}$ in this figure, if $\alpha=0$ we have $P(t)=\cos(\Delta t)$

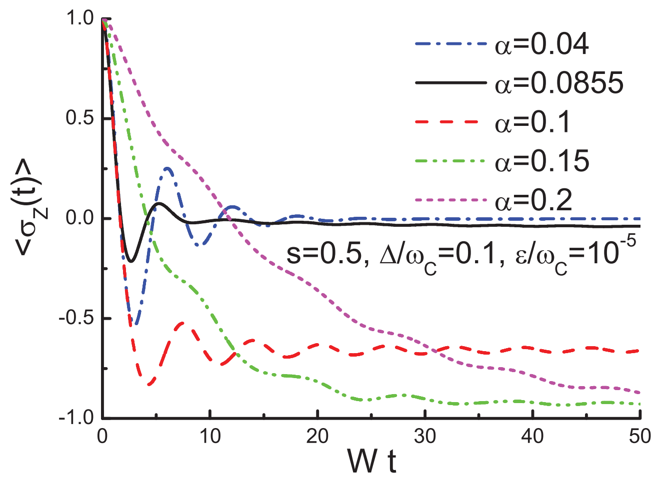

FIG. 9. (Color online) The time evolution of $P(t) = \langle\sigma_z(t)\rangle$ for $s = 1/2$, $\Delta/\omega_c = 0.1$, $\epsilon/\omega_c = 10^{-5}$, and several values of α.

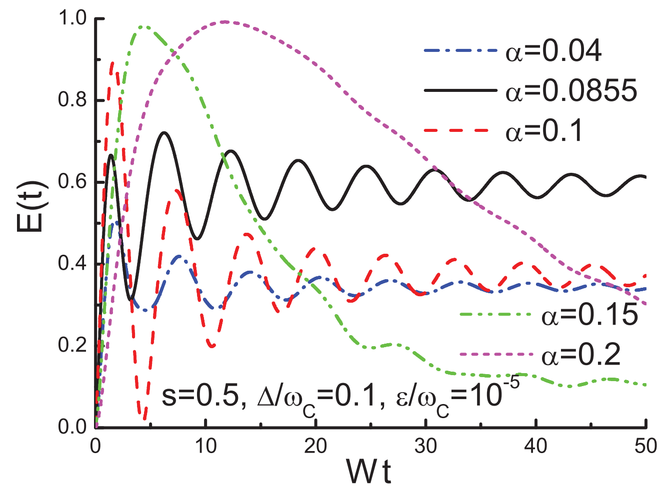

FIG. 10. (Color online) The time evolution of entanglement entropy for the same parameters as those of Fig. 9.

and it is the unattenuated Rabi oscillation with full quantum coherence. For weak coupling $\alpha = 0.04$ (dashed-dotted line), the Rabi oscillation and quantum coherence may be kept for some time. But for coupling $\alpha = 0.0855$ at the transition point (solid line), the Rabi oscillation proceeds for a shorter time. Note that for $\alpha \leqslant \alpha_c = 0.0855$, the long-time limit of $P(t)$ is $P(\infty) \approx 0$ as the renormalization effect of the dissipative interaction on the effective bias is very weak.

For $\alpha = 0.1 > \alpha_c$ (dashed line in Fig. 9), $P(t)$ starts from the initial value $P(0) = 1$, quickly decreases to its long-time limit $P(\infty) = \langle\sigma_z\rangle_G = -0.6564$ (see Fig. 5), and then weakly oscillates around $P(\infty)$. Here $P(\infty)$ is determined by the renormalization effect of the dissipative interaction. For $\alpha = 0.15$ [dashed-double-dotted line with $P(\infty) = -0.9276$] and $\alpha = 0.2$ [short-dashed line with $P(\infty) = -0.9722$], the renormalization effect of the dissipative interaction makes $P(t)$ largely biased with very weak oscillation without coherence.

From Fig. 9, we conclude that when $\alpha < \alpha_c \approx 0.0855$, the time evolution of $P(t)$ is coherent [26] with the long-time limit in the delocalized state. When $\alpha > \alpha_c$, the quantum dynamics of $P(t)$ is decoherent and its long-time limit goes down to the localized state.

The dynamic evolution of entanglement entropy for the same parameters as those of Fig. 9 is shown in Fig. 10. At $t = 0$, there is no entanglement between the two-level system and environment [$E(0) = 0$] because of the initial preparation. If $\alpha = 0$, we have $E(t) \equiv 0$ for all $t > 0$. For $\alpha \leqslant \alpha_c$, the entanglement goes up and then oscillates around its long-time limit [$E(\infty) = E(G)$] for some time (dashed-dotted line for $\alpha = 0.04$ and solid line for $\alpha = 0.0855$). When $\alpha = 0.1 > \alpha_c$ (dashed line in Fig. 10), the entanglement oscillates with large amplitude at the beginning and then decays quickly to its long-time limit $E(\infty) = E(G) = 0.3737$ (see Fig. 4). For $\alpha = 0.15$ [dashed-double-dotted line with $E(G) = 0.1063$] and $\alpha = 0.2$ [short-dashed line with $E(G) = 0.0424$], at the beginning the entanglement goes up to a maximum quite close to 1 and then decays with very weak oscillation to the long-time limit.

V. CONCLUDING REMARKS

The ground state and the spectral structure of lower-lying excited states of a dissipative two-level system coupled to a sub-Ohmic bath ($s = 1/2$) with nonzero bias have been studied using the method of unitary transformation. By calculating the ground-state average of σ_z, the ground-state entanglement entropy, and the static susceptibility of the two-level system, we have explored the nature of the transition (crossover) between the delocalized and localized state of the two-level system. Furthermore, we have calculated the time-dependent expectation $\langle\sigma_z(t)\rangle$ and the time evolution of the entanglement entropy to show that, when the system undergoes a transition (crossover) from a delocalized to a localized state, the time evolution of the two-level system changes from coherent to decoherent dynamics.

The main approximation in our treatment is the omission of $\tilde{H}_2$. Because of the functional form of η in Eq. (9), the operators in $\tilde{H}_2$ are in normal ordering and the lowest-order terms in $\tilde{H}_2|\tilde{G}\rangle$ are of the form $\alpha_k\alpha_{k'}b_k^\dagger b_{k'}^\dagger|\tilde{G}\rangle$. Thus, what we dropped are these multiboson nondiagonal transitions, and their contributions to the ground-state energy and other ground-state averages are $O(g_k^2 g_{k'}^2)$. We would emphasize that all diagonal bosonic transitions (to all orders) are taken into account with the factor η [27]. Because of our treatment, we believe that in the zero-temperature case, the contributions from these multiboson nondiagonal transitions may be dropped safely. The justifications of this approximation are as follows: (i) The ground-state energy of this work is lower than that of previous papers. (ii) The entanglement entropy of the ground state calculated in this work is in good agreement with that of the NRG [8]. (iii) The Shiba relation is satisfied.

ACKNOWLEDGMENTS

This work was supported by the National Basic Research Program of China (Grant No. 2011CB922202) and the National Natural Science Foundation of China (Grant No. 10734020).

[1] A. J. Leggett, S. Chakravarty, A. T. Dorsey, M. P. A. Fisher, A. Garg, and W. Zwerger, Rev. Mod. Phys. **59**, 1 (1987).
[2] U. Weiss, *Quantum Dissipative Systems* (World Scientific, Singapore, 1999).
[3] M. Sassetti and U. Weiss, Phys. Rev. Lett. **65**, 2262 (1990).
[4] M. Sassetti and U. Weiss, Phys. Rev. A **41**, 5383 (1990).
[5] T. A. Costi and R. H. McKenzie, Phys. Rev. A **68**, 034301 (2003).
[6] T. Stauber and F. Guinea, Phys. Rev. A **73**, 042110 (2006).
[7] A. Kopp and K. LeHur, Phys. Rev. Lett. **98**, 220401 (2007).
[8] K. LeHur, P. Doucet-Beaupre, and W. Hofstetter, Phys. Rev. Lett. **99**, 126801 (2007).
[9] S. K. Kehrein and A. Mielke, Phys. Lett. A **219**, 313 (1996).
[10] T. Stauber and A. Mielke, Phys. Lett. A **305**, 275 (2002).
[11] A. Chin and M. Turlakov, Phys. Rev. B **73**, 075311 (2006).
[12] A. Winter, H. Rieger, M. Vojta, and R. Bulla, Phys. Rev. Lett. **102**, 030601 (2009).
[13] R. Bulla, N. H. Tong, and M. Vojta, Phys. Rev. Lett. **91**, 170601 (2003).
[14] R. Bulla, H. J. Lee, N. H. Tong, and M. Vojta, Phys. Rev. B **71**, 045122 (2005).
[15] M. Vojta, N. H. Tong, and R. Bulla, Phys. Rev. Lett. **94**, 070604 (2005).
[16] F. B. Anders, R. Bulla, and M. Vojta, Phys. Rev. Lett. **98**, 210402 (2007).
[17] C. Gan and H. Zheng, Phys. Rev. E **80**, 041106 (2009).
[18] Z. Lu and H. Zheng, Phys. Rev. B **75**, 054302 (2007).
[19] H. Zheng, Eur. Phys. J. B **38**, 559 (2004).
[20] R. Silbey and R. A. Harris, J. Chem. Phys. **80**, 2615 (1984).
[21] D. P. S. McCutcheon, A. Nazir, S. Bose, and A. J. Fisher, Phys. Rev. B **81**, 235321 (2010).
[22] P. W. Anderson, Phys. Rev. **124**, 41 (1961).
[23] M. Keil and H. Schoeller, Phys. Rev. B **63**, 180302 (2001).
[24] H. Shiba, Prog. Theor. Phys. **54**, 967 (1975).
[25] W. H. Louisell, *Quantum Statistical Properties of Radiation* (Wiley, New York, 1973).
[26] R. Egger, H. Grabert, and U. Weiss, Phys. Rev. E **55**, R3809 (1997).
[27] G. D. Mahan, *Many-Particle Physics* (Plenum, New York, 1990), Chap. 6.